Title	Resist-substrate interface tailoring for generating high density arrays of Ge and Bi2Se3 nanowires by electron beam lithography
Authors	Hobbs, Richard G.;Schmidt, Michael;Bolger, Ciara T.;Georgiev, Yordan M.;Fleming, Peter G.;Morris, Michael A.;Petkov, Nikolay;Holmes, Justin D.;Xiu, Faxian;Wang, Kang L.;Djara, Vladimir;Yu, Ran;Colinge, Jean-Pierre
Publication date	2012-06-06
Original Citation	HOBBS, R. G., SCHMIDT, M., BOLGER, C. T., GEORGIEV, Y. M., FLEMING, P., MORRIS, M. A., PETKOV, N., HOLMES, J. D., XIU, F., WANG, K. L., DJARA, V., YU, R. & COLINGE, J.-P. 2012. Resist–substrate interface tailoring for generating high-density arrays of Ge and Bi2Se3 nanowires by electron beam lithography. Journal of Vacuum Science & Technology B, 30, 041602(1)-041602(7). doi: 10.1116/1.4724302
Type of publication	Article (peer-reviewed)
Link to publisher's version	http://scitation.aip.org/content/avs/journal/jvstb/30/4/10.1116/1.4724302 - 10.1116/1.4724302
Rights	© 2012 American Vacuum Society. This article may be downloaded for personal use only. Any other use requires prior permission of the author and AIP Publishing. The following article appeared in Journal of Vacuum Science & Technology B, 30:4, 041602 (2012) and may be found at http://scitation.aip.org/content/avs/journal/jvstb/30/4/10.1116/1.4724302
Download date	2024-05-03 04:48:16
Item downloaded from	https://hdl.handle.net/10468/2801

University College Cork, Ireland
Coláiste na hOllscoile Corcaigh

Resist–substrate interface tailoring for generating high-density arrays of Ge and Bi_2Se_3 nanowires by electron beam lithography

Richard G. Hobbs, Michael Schmidt, Ciara T. Bolger, Yordan M. Georgiev, Peter Fleming, Michael A. Morris, Nikolay Petkov,[a] and Justin D. Holmes[a]
Materials Chemistry and Analysis Group, Department of Chemistry and the Tyndall National Institute, University College Cork, Cork, Ireland and Centre for Research on Adaptive Nanostructures and Nanodevices (CRANN), Trinity College Dublin, Dublin 2, Ireland

Faxian Xiu and Kang L. Wang
Department of Electrical Engineering, University of California–Los Angeles, Los Angeles, California, 90095

Vladimir Djara, Ran Yu, and Jean-Pierre Colinge
Silicon Research Group, Tyndall National Institute, Lee Maltings, Prospect Row, Ireland

(Received 21 December 2011; accepted 8 May 2012; published 6 June 2012)

The authors report a chemical process to remove the native oxide on Ge and Bi_2Se_3 crystals, thus facilitating high-resolution electron beam lithography (EBL) on their surfaces using a hydrogen silsesquioxane (HSQ) resist. HSQ offers the highest resolution of all the commercially available EBL resists. However, aqueous HSQ developers such as NaOH and tetramethylammonium hydroxide have thus far prevented the fabrication of high-resolution structures via the direct application of HSQ to Ge and Bi_2Se_3, due to the solubility of components of their respective native oxides in these strong aqueous bases. Here we provide a route to the generation of ordered, high-resolution, high-density Ge and Bi_2Se_3 nanostructures with potential applications in microelectronics, thermoelectric, and photonics devices. © *2012 American Vacuum Society*. [http://dx.doi.org/10.1116/1.4724302]

I. INTRODUCTION

Hydrogen silsesquioxane (HSQ) is a high-resolution, negative-tone, inorganic, electron beam lithography (EBL) resist, which is capable of producing high-density features in the sub-20 nm regime.[1,2] Additionally, following electron beam exposure, HSQ physically and chemically, closely resembles SiO_2.[3] This similarity to SiO_2 ensures that HSQ is inherently compatible with current microelectronics processing. To date, the use of HSQ has been largely limited to Si processing, although the application of HSQ to several other materials has been reported.[4–6]

This article describes the application of an HSQ EBL process to single crystal Ge wafers, and Ge and Bi_2Se_3 thin films grown by molecular beam epitaxy (MBE). Literature reports on the application of an HSQ EBL process to these materials have detailed difficulties with the direct application of HSQ to their surfaces, and have attributed these difficulties to poor adhesion between HSQ and the surfaces of the materials. Consequently, there have been a number of reports identifying "adhesion promoting" interstitial layers such as Ti,[5] Si,[7] and Cr.[8] This work identifies the cause of the reported "poor adhesion" and further concludes that, although HSQ does in fact adhere well to the surfaces of Ge and Bi_2Se_3, it is in fact the high solubility of the native oxides of these materials in the aqueous, basic, HSQ developer solutions that results in delamination of HSQ structures from the respective surfaces of Ge and Bi_2Se_3. The present work not only identifies why the need for HSQ adhesion promoters exists, but also details routes to apply HSQ directly to the surfaces of Ge and Bi_2Se_3, without the use of additional adhesion promoting layers. Adhesion promoting layers, such as those detailed previously, may not be compatible with all processes, e.g., metallization is typically avoided prior to device contact formation in front end of line lithography for integrated circuit fabrication. Further, the presence of additional adhesion promoting layers introduces the requirement for additional etching steps both prior to, and following pattern transfer to the device layer. Consequently, a technique such as that detailed herein may find favor when high-resolution lithography is required directly on Ge or Bi_2Se_3 surfaces or when a process compatible adhesion promoting layer does not exist.

Ge is an intrinsic group 14 semiconductor that offers a number of distinct advantages over Si for microelectronic device applications.[9,10] Namely, Ge exhibits superior electron and hole mobilities relative to Si and has a lower band gap energy.[11] Ge possesses a complex native oxide (GeO_x) consisting of GeO and GeO_2 components, as well as nonstoichiometric oxides. Both GeO and GeO_2 are soluble in tetramethylammonium hydroxide (TMAH) and NaOH. Consequently, if a GeO_x layer exists between the Ge crystal and the HSQ EBL resist, dissolution of the underlying GeO_x layer during development of the resist will result in lift-off of any high-resolution features written by EBL. Removal of the native Ge oxide is thus imperative prior to HSQ deposition, to facilitate the use of traditional aqueous HSQ developers. Although nonaqueous developers do exist for HSQ, these have been shown to offer significantly lower resolution than their aqueous counterparts.[12]

Bi_2Se_3 has attracted much attention due to recently discovered topological insulating properties in the material.[13,14]

[a]Authors to whom correspondence should be addressed; electronic addresses: nikolay.petkov@tyndall.ie; j.holmes@ucc.ie

Topological insulator nanowires and nanoribbons may have applications in quantum computing.[15] Bi_2Se_3 has also been extensively studied for thermoelectric devices and infrared detector applications.[16] Hicks and Dresselhaus proposed in the early 1990s that one-dimensional (1D) thermoelectric materials would display enhanced thermoelectric performance relative to bulk materials, due to reduced thermal conductivity in the 1D structures caused by confinement effects on the mean free path of phonons in the confined material. As a result, 1D thermoelectric materials, such as Bi_2Se_3 nanowires and nanoribbons, have been increasingly researched as potentially useful materials in next generation thermoelectric generators.[17] Kong *et al*. recently showed that the native oxide on Bi_2Se_3 is composed of both BiO_x and SeO_x, and although the BiO_x component rapidly forms on oxide free Bi_2Se_3 surfaces, the SeO_x component forms slower.[18] Importantly, at room temperature, the SeO_x component of the native oxide is soluble in aqueous bases, whereas the BiO_x component is not.[19] Consequently, application of an HSQ EBL process to Bi_2Se_3 requires removal of SeO_x prior to HSQ deposition. This work thus details a reproducible route to the production of high-resolution features on Ge and Bi_2Se_3 using an HSQ direct-write, negative-tone, EBL process.

II. EXPERIMENT

Ge substrates were patterned using the following approach. A 15 mm × 15 mm piece of *p*-doped (P, 10^{17} cm^{-3}) or *n*-doped (As, 10^{17} cm^{-3}) Ge ⟨100⟩ oriented wafer was first degreased via ultrasonication in acetone and iso-propanol (IPA) solutions (2 × 2 min), dried in flowing N_2 gas and baked for 2 min at 120 °C in an ambient atmosphere to remove any residual IPA. Immediately prior to deposition of the HSQ resist layer the Ge surface was Cl terminated. The process used to achieve Cl termination was similar to that reported by Sun *et al*.[20] First, the Ge wafer was immersed in de-ionized (DI) water for 30 s, and then 4.5 M HNO_3 for 30 s followed by drying in flowing N_2 gas for 15 s. The Ge piece was then immersed in a 10 wt. % HCl solution for 10 min. The wafer was then dried in flowing N_2 for 10 s, and spin-coated (2000 rpm, 32 s, lid closed) with a 1.2 wt. % solution of HSQ (XR-1541 Dow Corning Corp.) in methylisobutyl ketone (MIBK) to produce a 25 nm film of HSQ. The wafer was baked at 120 °C in an ambient atmosphere for 3 min prior to transfer to the EBL system for exposure. The pre-exposure bake served two purposes: (i) the HSQ oligomers in the resist film thermally increase in size due to cross-linking during baking, thus lowering the required electron dose for high-resolution EBL, and (ii) baking removes any residual MIBK solvent. Electron beam exposure was performed using a Zeiss Supra 40 FESEM equipped with a Raith Elphy digital pattern generator operating at 10 keV. All Ge samples were developed in a 0.125 M NaOH, 0.35 M NaCl solution for 30 s followed by a rinse in flowing DI water for 60 s. The samples were then dried in flowing N_2 gas. A Cl_2 reactive ion etch (RIE) was performed in an Oxford Instruments Plasmalab 100, to transfer the HSQ pattern to the underlying Ge substrate. Process parameters used for the Cl_2 RIE included a Cl_2 flow rate of 30.0 SCCM (where SCCM denotes cubic centimeters per minute at standard temperature and pressure), radio frequency power of 80 W, 10 mTorr working pressure, 20 °C substrate temperature, and a 10 s etch time. Further, the sample to be etched was thermally contacted to the stage of the RIE tool via a thin layer of *Cool-Grease* (Amerasia International Technology Inc.) applied to the underside of the sample.

MBE-grown Bi_2Se_3 thin films were produced as described previously.[21] Prior to HSQ deposition the native oxide on the Bi_2Se_3 films was dissolved by immersing the substrate in an aqueous solution of 0.25 v/v developer/DI water, 0.023 M TMAH, 0.006 M NaOH, and 0.016 M NaCl, for 15 s, rinsed in flowing DI water for 30 s, and dried in flowing N_2 gas for 10 s. A 1.2 wt. % HSQ solution was immediately dispersed on the substrate and spin-coated as described previously. The sample was then baked at 120 °C in an ambient atmosphere for 3 min prior to transferring to the EBL system for exposure. The sample was developed by manual immersion in an aqueous developer solution of 0.116 M TMAH, 0.028 M NaOH, and 0.078 M NaCl for 15 s, rinsed in flowing DI water for 60 s, and dried in a flow of N_2 gas for 15 s. The HSQ pattern was transferred to the Bi_2Se_3 film using an Ar^+ ion etch in an Oxford Instruments Plasmalab 100.

Scanning electron microscopy (SEM) was performed on a Zeiss Supra 40 FESEM. Transmission electron microscopy (TEM) cross sections were prepared using a standard focused ion beam (FIB) mill and lift-out technique on a FEI Helios Nanolab 600i dual-beam SEM/FIB equipped with an Omniprobe micromanipulator. TEM analysis was performed on a Jeol 2010 high-resolution instrument with a LaB_6 emission source operating at 200 kV.

III. RESULTS

Cl-terminated Ge was found to successfully eliminate the presence of an interfacial Ge oxide between the Ge substrate and the HSQ EBL resist. Elimination of the native oxide on Ge thus allowed for the production of ordered arrays of 20 nm wide HSQ lines directly onto the Ge surface. Figure 1 shows an SEM micrograph of 20 nm wide HSQ lines produced on Cl-terminated *p*-Ge. Figure 1 (inset) is an SEM micrograph of a Ge sample for which the native oxide was not removed prior to HSQ deposition and EBL exposure. Comparing the two SEM micrographs in Fig. 1, it is apparent that removal of the native Ge oxide prior to EBL is necessary to produce ordered arrays of high-resolution HSQ features on Ge surfaces. The requirement for removal of the native Ge oxide prior to EBL processing can be attributed to the high solubility of GeO_2, and to a lesser extent GeO, in strong aqueous bases such as NaOH. When the sample shown in Fig. 1 (inset) was placed in the developer solution after electron beam exposure, the native Ge oxide between the Ge crystal and the exposed HSQ was dissolved. Dissolution of the native Ge oxide in the developer solution resulted in partial lift-off of the HSQ lines and consequently a loss of

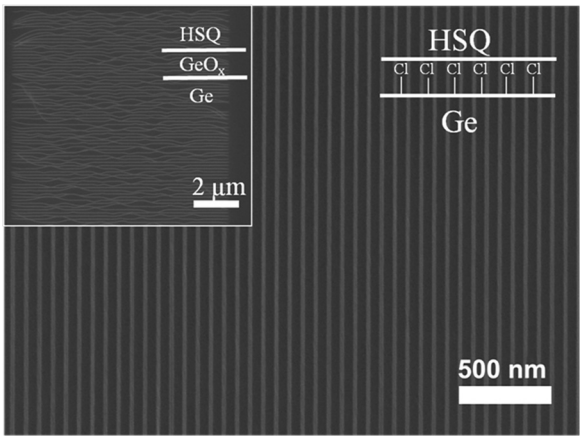

FIG. 1. HSQ lines, 20 nm wide, at a pitch of 70 nm, written on a Ge ⟨100⟩ substrate at an area dose of 900 μC cm^{-2}. (Inset) HSQ lines, 20 nm wide, at a pitch of 70 nm, written on a Ge ⟨100⟩ (GeOx surface) substrate at an area dose of 900 μC cm^{-2}.

order in the resultant HSQ mask as shown in the SEM micrograph in Fig. 1 (inset). Line edge roughness (LER) of the 20 nm wide HSQ lines (pitch 70 nm) was measured at 3.3 nm (3σ) by analysis of high magnification SEM images using IMAGEJ software. Details of the process used to calculate LER are included in the supplementary material.[22]

Figure 2 shows Ge 3dd core level XPS spectra for Ge samples before and after chemical treatment to remove the native Ge oxides. The Ge 3*d* peak has been deconvoluted to reveal the contributions from the $3d_{5/2}$ and $3d_{3/2}$ levels in Ge^0, as well as higher oxidation states of Ge. Prior to chemical treatment to remove the native oxide there is an observed broadening of the Ge 3*d* core level peak (FWHM 2.48 eV) due to the contribution from GeO_x, which results in additional blueshifted Ge 3*d* peaks relative to bulk Ge^0. After chemical treatment to remove the native Ge oxides the Ge 3*d* core level peak was observed to narrow (FWHM 2.08 eV) as the contribution from higher oxidation states of Ge is removed. Similarly, there was a significant change in the O 1*s* core level spectrum (Fig. S2, in Ref. 22) before and after chemical treatments to remove the native oxide. Although there is a clear O 1*s* peak observed at ~532 eV in the sample prior to chemical treatment, any signal due to O 1*s* was below the level of the background noise of the spectrum after chemical treatment to remove the native oxide. The HSQ pattern produced using the process outlined previously, was subsequently transferred to a *p*-Ge substrate using a Cl_2 RIE. An example of a sample where the pattern was transferred to the substrate is shown in Fig. 3. Figure 3 shows an SEM micrograph of 15 nm wide Ge fins at a pitch of 120 nm. Details of electron exposure doses for the HSQ mask used to produce these structures are included in the supporting information (Fig. S3).[22] The fins have been etched into the Ge wafer to a depth of 20 nm. Figure 3 (inset) is an HRTEM micrograph of a cross section of a 15 nm wide fin. The fin shown in the HRTEM micrograph in Fig. 1 was purposely produced along a ⟨110⟩ zone axis of the Ge crystal. The family of ⟨110⟩ axes are known to offer the highest charge carrier mobility within *p*-type Ge (*Fd3m* crystal system), and are thus preferable for device fabrication.[23]

Fabrication of arrays of high-resolution HSQ lines on a Ge wafer using the HSQ EBL process, outlined previously, was also observed to depend on the age of the HSQ resist. HSQ has a shelf life of 6 months when stored in a sealed container at 5 °C. We have observed that the process for

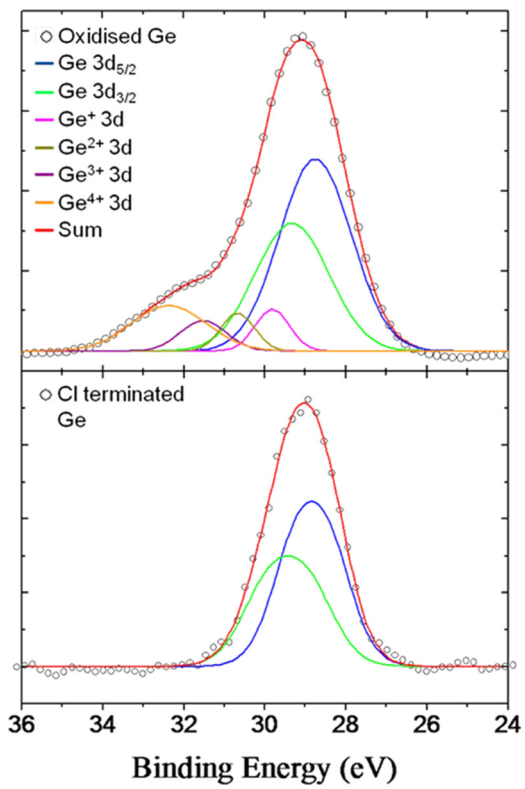

FIG. 2. (Color online) Ge 3*d* core-level XPS spectra of a ⟨100⟩ Ge wafer before (upper spectrum) and after (lower spectrum) chemical treatment to remove the native oxide. The untreated wafer exhibited significant peak broadening and a blueshifted shoulder consistent with the presence of a native Ge oxide at the surface of the sample.

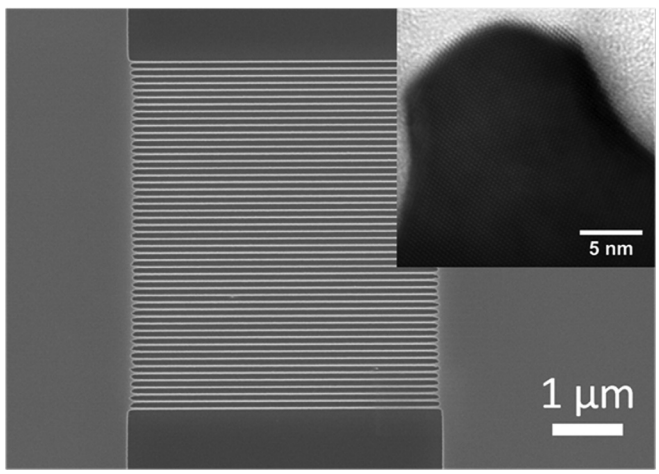

FIG. 3. Ge fins, 15 nm wide, at a pitch of 120 nm, etched to a depth of 20 nm. Fin length is 4.5 μm and fins are integrated with Ge pads (shown left and right) in device-ready architecture. (Inset) A TEM micrograph displaying a cross section of one such 15 nm wide Ge fin.

producing high-resolution HSQ lines on Ge is reproducible and repeatable up to ~1 month after the stated expiry date. However, after this time, effects like those shown in Fig. 1 (inset) were observed, where exposed lines partially delaminate from the substrate during development. This observation suggests that the Si–H groups in the HSQ resist play an important role in the adhesion of the HSQ resist to the Cl-terminated Ge surface. As the HSQ resist ages, the cage-like oligomers within the resist cross-link forming a network structure with the evolution of hydrogen gas. The Si–H sites in HSQ have been reported to be the sites involved in HSQ cross-linking and network formation.[24] Consequently, as the resist ages fewer Si–H sites are available to interact with the substrate to which the resist is applied. The fact that delamination of electron beam exposed HSQ lines from chlorinated Ge substrates is observed when HSQ ages beyond a certain point is thus indicative of cross-linking of the resist to the substrate.

Fourier transform infrared (FTIR) spectroscopy was used to investigate the presence of any chemical interaction between the HSQ resist and a Cl-terminated Ge substrate (Fig. S4[22]), following electron beam exposure or thermal treatment. Figure S4[22] shows an FTIR spectrum of a 25 nm HSQ film deposited on a 20 nm Ge film prepared on a Si substrate by MBE (Ge–Si) prior to electron beam exposure or thermal annealing. Preparation of the Ge–Si substrates has been described elsewhere, and TEM analysis has confirmed the highly crystalline epitaxial interface between the Ge film and the Si substrate.[25] The native Ge surface oxide was removed, and the Ge film was terminated with Cl prior to HSQ deposition. The spectrum in Fig. S4[22] was produced by subtracting the spectrum produced by a clean Ge–Si substrate from that of a Ge–Si substrate coated with a 25 nm HSQ film. The spectrum in Fig. S4[22] shows the hallmark absorbance peaks associated with HSQ. The Si–H stretch is observed at 2256 cm^{-1}, which is characteristic of a Si–H species, whereby the Si atom is bound to three electronegative O atoms leading to a blueshift in the Si–H absorbance peak relative to an Si–H species present on a hydride terminated Si wafer, for example. The asymmetric Si–O–Si stretching modes for cage and network HSQ structures have absorbance peaks labeled $\nu_{as}(Si–O–Si)_{cage}$ and $\nu_{as}(Si–O–Si)_{net}$ and are visible at 1122 and 1065 cm^{-1}, respectively, whereas Si–O bending modes are observed at 860 and 827 cm^{-1} and are labeled d(H–Si–O) and d(O–Si–O), respectively. The bending modes d(H–Si–O) and d(O–Si–O) can be attributed to the cage and network structures, respectively, as reported previously.[26,27] The greater intensity of the $\nu_{as}(Si–O–Si)_{cage}$ and d(H–Si–O) absorbance peaks in Fig. S4[22] with respect to the $\nu_{as}(Si–O–Si)_{net}$ and d(O–Si–O) peaks, respectively, is consistent with a high concentration of the cage species with respect to that of the network analog prior to electron beam exposure or high temperature thermal treatment.

Figure 4 displays FTIR spectra of 25 nm HSQ films on Ge–Si and Si substrates after annealing at 673 K for 1 h in a N_2 atmosphere. The HSQ changes upon heating are typical of the literature. Here we note that there is the addition of a

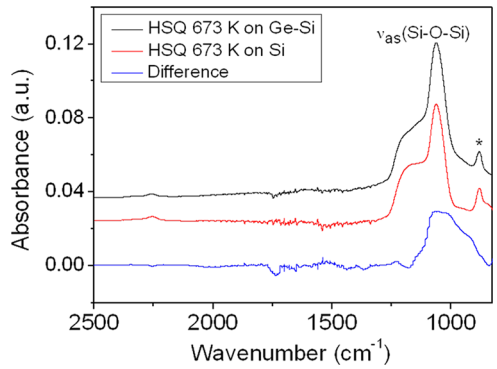

FIG. 4. (Color online) FTIR spectra of 25 nm HSQ films deposited on an MBE-grown Ge thin film (top trace), and a Si substrate (middle trace) annealed in a N_2 atmosphere at 673 K. The peak labeled with an asterisk (*) is associated with a Si–O bending mode in a Si rich oxide. The bottom trace represents the difference between the middle and top traces after baseline correction, and the broad absorption peak at ~1000 cm^{-1} can be attributed to a combination of Si–O–Si and Ge–O–Si moieties. Spectra are offset arbitrarily along the absorbance axis for clarity.

Ge–O–Si peak, which we attribute to chemical bonding at the interface. This did not appear in electron beam exposed samples possibly due to insufficient signal. We expect its presence due to the potential for a condensation reaction at the interface between the Si–H bonds in the HSQ and Cl terminated Ge as highlighted in the upcoming Eq. (1). The peaks associated with the cage structure of HSQ seen in Fig. S4[22] are notably absent from the spectra in Fig. 4, these include the Si–H stretch, $\nu_{as}(Si–O–Si)_{cage}$, and d(H–Si–O) at 2256, 1122, and 860 cm^{-1}, respectively. The dominant feature of the spectra in Fig. 4 is the absorbance peak at 1060 cm^{-1}, associated with asymmetric stretching of the Si–O–Si moiety in a SiO_2 glass. Another feature present in the FTIR spectra of the HSQ films on Ge–Si and Si shown in Fig. 4, is the peak denoted with an asterisk (*) at 879 cm^{-1} associated with a Si–O bending mode in a Si rich silicon oxide.[27] The bottom trace in Fig. 4 represents the difference between the middle and top traces and shows a broad peak centered at ~1000 cm^{-1}, which can be partially attributed to the presence of a Ge–O–Si moiety.[28,29] Formation of a Ge–O–Si linkage between the HSQ resist and the Ge crystal during cross-linking of the HSQ resist by thermal treatment or electron beam exposure would further increase resist adhesion to the Ge substrate and prevent pattern lift-off in the developer solution. The formation of a Ge–O–Si linkage may thus allow resist features with smaller critical dimensions to be produced on Ge than in the absence of such a covalent linkage.

Similar FTIR analyses were also performed on electron beam exposed HSQ films on Si and Ge–Si substrates. A 2 mm × 1.5 mm area was exposed at a dose of 800 $\mu C\ cm^{-2}$ on 25 nm HSQ films on both Si and Ge–Si substrates, requiring an exposure time of 48 h each. Figure S5[22] shows FTIR spectra obtained from the exposed and developed HSQ films on both Si and Ge–Si substrates. The spectra shown in Fig. S5[22] very closely resemble those of the annealed HSQ films, shown in Fig. 4. The most significant peaks in the spectra in Fig. S5[22] are the same as those highlighted in Fig. 4,

those being the asymmetric Si–O–Si stretch at 1060 cm^{-1} and the Si–O bend at 879 cm^{-1}. When the difference between the FTIR spectra obtained from the electron beam exposed samples was considered bottom trace in Fig. S5,[22] only a very low intensity absorbance peak at 1030 cm^{-1} consistent with a Ge–O–Si vibrational mode[29] was observed, however, this peak is almost at the noise level of the spectrum. Electron beam exposure of a larger area of HSQ film may facilitate detection of a more significant signal from the HSQ interface with Ge, however, this would require electron beam exposure times of a week or more for each of the Si and Ge–Si samples. Electron beam exposure and thermal curing of HSQ films have been shown previously to result in similar Si–H and Si–O bond redistribution effects, thus, thermal curing can be considered to produce comparable effects to electron beam exposure in HSQ films.[3,30] Consequently, the Ge–O–Si moiety observed in HSQ films deposited on Cl-terminated Ge after thermal curing suggests that HSQ patterns produced on Cl-terminated Ge by EBL are covalently bound to the Ge crystal, thus preventing lift-off of high-resolution HSQ patterns during HSQ development. Direct cross-linking of HSQ films to the Cl-terminated Ge substrate is likely to be a dynamic process involving the hydrolysis of the Ge–Cl species by residual water remaining from the aqueous HCl solution used to chlorinate the Ge surface. Ge–OH species formed by hydrolysis of Ge–Cl would readily react with silanol groups present in the HSQ films during thermal annealing or electron beam exposure resulting in the formation of Ge–O–Si linkages via a condensation reaction as shown in the following equation[28]:

$$\mathrm{Ge_{bulk}–Ge–OH + HO–Si–HSQ_{network}} \rightarrow \mathrm{Ge_{bulk}–Ge–O–Si–HSQ_{network} + H_2O}. \quad (1)$$

Figure 5(a) shows an SEM image of a cubic array of 20 nm diameter Bi_2Se_3 disks at a pitch of 100 nm. Figure 5(b) displays an SEM image of 30 nm wide and 2 nm thick Bi_2Se_3 nanoribbons produced using the HSQ EBL process outlined previously. The HSQ etch mask remains on top of the Bi_2Se_3 structures in Figs. 5(a) and 5(b). Figures 5(c) and 5(d) show a comparison of HSQ lines exposed on an untreated Bi_2Se_3 surface [Fig. 5(c)] and a Bi_2Se_3 surface that has been washed with a NaOH/TMAH solution to dissolve surface SeO_2 [Fig. 5(d)]. Comparing Figs. 5(c) and 5(d), it is again apparent that the presence of a surface oxide, which is soluble in the HSQ developer, inhibits the production of ordered arrays of high-resolution HSQ structures using an HSQ EBL process.

Figure 6 displays a selection of cross-sectional TEM micrographs of Bi_2Se_3 nanoribbons produced from a 7 nm Bi_2Se_3 film grown by MBE. The Bi_2Se_3 film was patterned using the HSQ EBL process outlined previously and the pattern was transferred to the film using an Ar^+ ion etch. Figure 6(a) displays 30 nm wide nanoribbons at a pitch of 60 nm produced from an 8 nm thick Bi_2Se_3 film. Figure 6(b) shows an HRTEM micrograph of the crystal lattice of a single Bi_2Se_3 nanoribbon. The HRTEM micrograph clearly shows the layered crystal structure of rhombohedral Bi_2Se_3 with the *c*-axis of the crystal oriented orthogonally to the Si ⟨111⟩ substrate. The repeating units in the layered structure of the Bi_2Se_3 thin films are known as quintuple layers (QL) and are stacked along the *c*-axis. Each QL is so-called as it consists of five layers of atoms in the sequence Se–Bi–Se–Bi–Se. Within each QL, strong covalent and ionic bonding dominates, however, only weak van der Waals-type bonding exists between the two Se layers at the QL–QL interface.[31] The observed QLs in Fig. 6(b) are ~1 nm thick as described in previous reports. The Bi_2Se_3 film thickness is an integer multiple of the QL period. Figure 6(c) shows an HRTEM micrograph of a cross section of an 18 nm wide, 7 nm thick, Bi_2Se_3 nanoribbon. An amorphous layer of material is observed at the interface between the nanoribbon (dark region) and the Si substrate

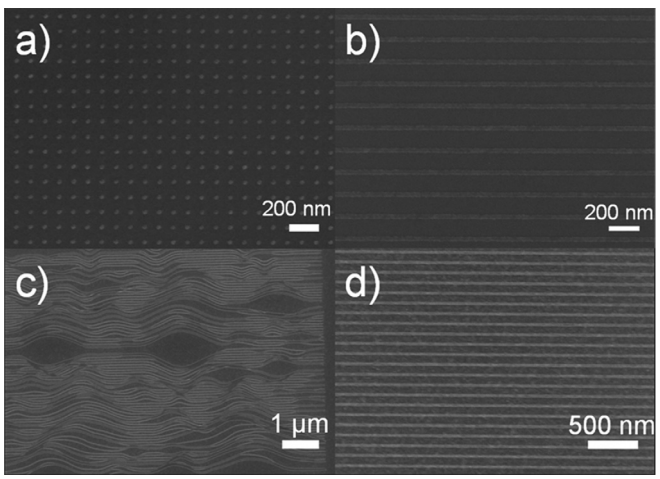

FIG. 5. (a) Cubic array of 20 nm diameter, 2 nm high Bi_2Se_3 disks at 100 nm pitch. (b) Bi_2Se_3 nanoribbons, 30 nm wide, at a pitch of 140 nm. (c) HSQ lines, 20 nm wide, exposed at a pitch of 70 nm on an untreated Bi_2Se_3 surface. (d) HSQ lines, 20 nm wide, exposed at a pitch of 100 nm on a Bi2Se_3 surface washed with a NaOH/TMAH solution prior to HSQ deposition to remove surface SeO_2.

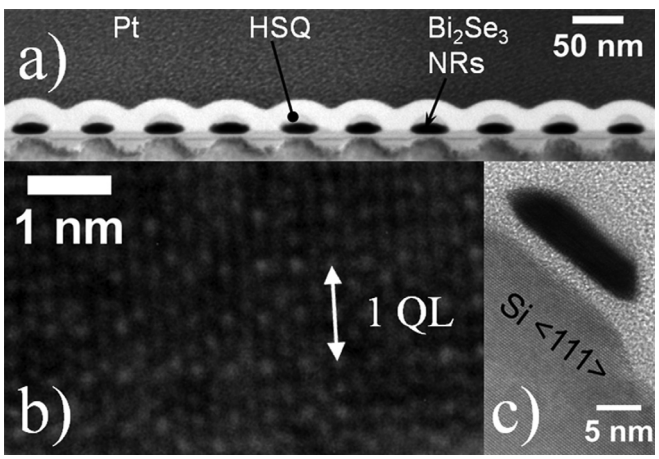

FIG. 6. (a) Cross-sectional TEM micrograph of 30 nm wide, 8 nm high, Bi_2Se_3 nanoribbons at a pitch of 60 nm. HSQ mask remains atop the Bi_2Se_3 nanoribbons. (b) HRTEM micrograph of a cross section of a Bi_2Se_3 nanoribbon. (c) HRTEM micrograph of a cross section through a Bi_2Se_3 nanoribbon and the underlying Si ⟨111⟩ substrate.

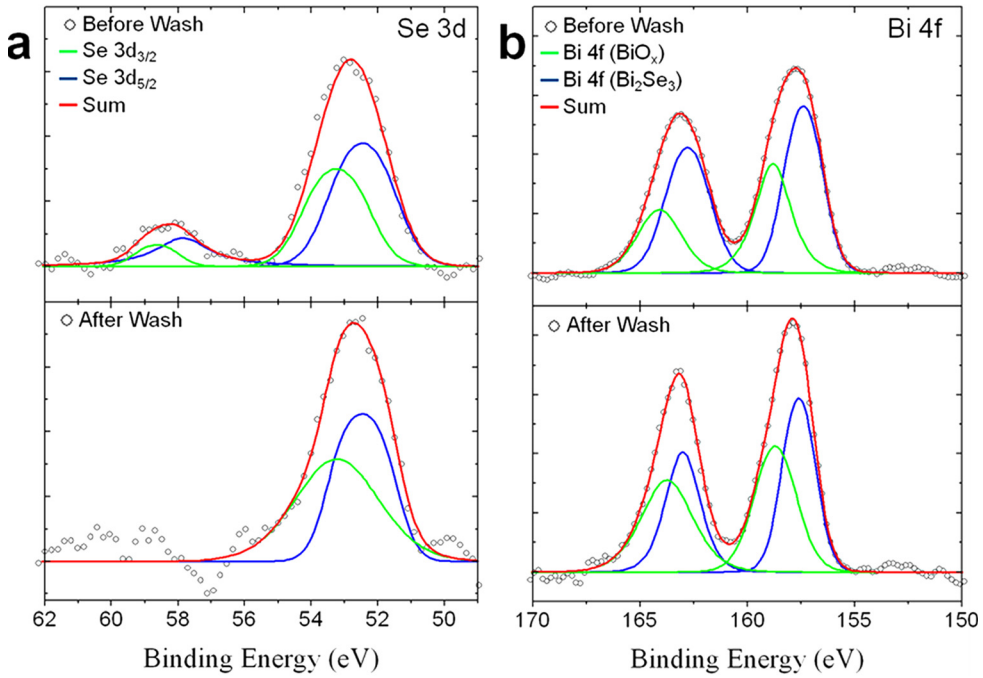

FIG. 7. (Color online) XPS core-level spectra of Bi_2Se_3 thin films before and after TMAH/NaOH/NaCl washing to remove SeO_2. (a) Se 3*d* core level XPS spectra showing a Se 3*d* peak attributable to Bi_2Se_3 at ~52.8 eV and a lower intensity peak attributable to SeO_2 at ~58.3 eV prior to washing. Top trace represents sum of the Se $3d_{3/2}$ (lower trace) and $3d_{5/2}$ (middle trace) peaks obtained through deconvolution of the raw data. (b) Bi 4*f* core level XPS spectra showing peaks attributable to the Bi $4f_{5/2}$ and $4f_{7/2}$ core levels at approximately 158 and 163 eV, respectively. Top trace represents sum of Bi $4f_{5/2}$ and $4f_{7/2}$ peaks from Bi_2Se_3 (middle trace) and Bi $4f_{5/2}$ and $4f_{7/2}$ peaks from Bi_2O_3 (lower trace).

(lower left) in Fig. 6(c), which can be attributed to the formation of a layer of amorphous SiO_2, which is formed following MBE Bi_2Se_3 thin film growth. Amorphous SiO_2 formation can be attributed to the diffusion of oxygen through the Bi_2Se_3 thin film when the Bi_2Se_3 film is exposed to an ambient atmosphere.[32]

XPS analysis of a Bi_2Se_3 thin film sample before and after treatment with the TMAH/NaOH/NaCl solution revealed a change in the composition of the surface of the sample. A Bi_2Se_3 thin film, which had been stored in a chemical dehumidifier at room temperature for 6 months while waiting for further processing, was analyzed by XPS as shown in the upper spectra in Fig. 7. Deconvolution of the Bi 4*f* core level peaks [upper spectrum Fig. 7(b)] revealed the presence of the $4f_{7/2}$ and $4f_{5/2}$ peaks from Bi_2Se_3 at 157.4 and 162.8 eV, respectively (peak area ratio of 1.32 measured for $4f_{7/2}/4f_{5/2}$). Further, the deconvolution reveals Bi $4f_{7/2}$ and $4f_{5/2}$ peaks blueshifted by 1.3 eV relative to the Bi 4*f* core level peaks attributed to Bi_2Se_3. These blueshifted peaks can be attributed to Bi interacting with a more electronegative species than Se, i.e., Bi_2O_3. The blueshift of 1.3 eV for Bi_2O_3 is consistent with recent observations reported for Bi_2Se_3 nanowires.[18] Comparison of the 4*f* core level peak areas for Bi_2Se_3 and Bi_2O_3 suggests a Bi_2Se_3/Bi_2O_3 ratio of 3/1. Consequently, when the relative densities of Bi_2Se_3 and Bi_2O_3 are considered, it can be inferred that the as-grown 8 nm thick Bi_2Se_3 film, should now exist as a 6 nm Bi_2Se_3 film capped with a 2 nm Bi_2O_3 layer. Figure 7 also shows XPS spectra of the Se component of the native oxide. The spectra shown in Fig. 7(a) display Se 3*d* core level peaks attributable to Se^{2-} in Bi_2Se_3 at a binding energy of 52.8 eV. Deconvolution of the peak at 52.8 eV reveals contributions from the Se $3d_{5/2}$ and $3d_{3/2}$ levels at binding energies of 52.4 and 53.2 eV, respectively, suggesting a crystal field splitting energy of 0.8 eV. The sample analyzed prior to washing with the TMAH/NaOH/NaCl solution, also revealed a lower intensity Se 3*d* core level peak at a binding energy of 58.3 eV. The blueshift of the peak attributed to SeO_2 relative to that attributed to Bi_2Se_3 is a consequence of the large difference in oxidation of Se in the two species in question, Se^{4+} in SeO_2 and Se^{2-} in Bi_2Se_3.

IV. SUMMARY AND CONCLUSIONS

To conclude, successful chemical routes to remove the native oxides of both Ge and Bi_2Se_3 prior to the application of HSQ EBL resist have been demonstrated. The chemical processing of Ge and Bi_2Se_3 described herein is imperative to produce ordered arrays of high-resolution nanostructures in both of these materials using an HSQ EBL process. Consequently, where a material possesses a native oxide, which is soluble in HSQ developers, the limiting factors to achieving high-resolution HSQ nanostructures on the surface of such a material, is the availability of a viable route to remove the native oxide and the adhesion of HSQ to the oxide-free surface of the underlying material.

Further, a route to the production of covalently bound SiO_x films on Ge has been demonstrated by thermal curing of HSQ films deposited on Cl-terminated Ge crystals. This route may find applications in the fabrication of Ge-on-insulator substrates, as well as in the production of low-*k* dielectric films on Ge materials.

ACKNOWLEDGMENTS

The authors acknowledge financial support from the Irish Research Council for Science, Engineering and Technology (IRCSET) and Science Foundation Ireland (Grant Nos. 08/CE/I1432, 09/IN.1/I2602, and 09/SIRG/I1621). This research was also enabled by the Higher Education Authority Program for Research in Third Level Institutions (2007-2011) via the INSPIRE program. The authors acknowledge Gillian Collins for assistance with ATR-FTIR measurements and Stephen Connaughton for initial Ar^+ ion etch tests on Bi_2Se_3 films.

[1]A. E. Grigorescu and C. W. Hagen, Nanotechnology **20**, 292001 (2009).
[2]W. Henschel, Y. M. Georgiev, and H. Kurz, J. Vac. Sci. Technol. B **21**, 2018 (2003).
[3]S. Choi, M. J. Word, V. Kumar, and I. Adesida, J. Vac. Sci. Technol. B **26**, 1654 (2008).
[4]W. Chao, J. Kim, S. Rekawa, P. Fischer, and E. Anderson, J. Vac. Sci. Technol. B **27**, 2606 (2009).
[5]D. S. Macintyre, I. Young, A. Glidle, X. Cao, J. M. R. Weaver, and S. Thoms, Microelectron. Eng. **83**, 1128 (2006).
[6]S. Ryu, M. Y. Han, J. Maultzsch, T. F. Heinz, P. Kim, M. L. Steigerwald, and L. E. Brus, Nano Lett. **8**, 4597 (2008).
[7]S.-W. Nam, T.-Y. Lee, J.-S. Wi, D. Lee, H.-S. Lee, K.-B. Jin, M.-H. Lee, H.-M. Kim, and K.-B. Kim, J. Electrochem. Soc. **154**, H844 (2007).
[8]J. Reinspach, F. Uhlen, H. M. Hertz, and A. Holmberg, J. Vac. Sci. Technol. B **29**, 06FG02 (2011).
[9]R. G. Hobbs, S. Barth, N. Petkov, M. Zirngast, C. Marschner, M. A. Morris, and J. D. Holmes, J. Am. Chem. Soc. **132**, 13742 (2010).
[10]J. Xiang, W. Lu, Y. Hu, Y. Wu, H. Yan, and C. M. Lieber, Nature (London) **441**, 489 (2006).
[11]S. M. Sze, *Semiconductor Devices: Physics and Technology*, 1st ed. (Wiley, New York, 1985).
[12]G. M. Schmid, L. E. Carpenter II, and J. Alexander Liddle, J. Vac. Sci. Technol. B **22**, 3497 (2004).
[13]D. Hsieh *et al.*, Nature (London) **460**, 1101 (2009).
[14]D. Kong *et al.*, Nano Lett. **10**, 329 (2010).
[15]J. E. Moore, Nature (London) **464**, 194 (2010).
[16]X. Qiu, L. N. Austin, P. A. Muscarella, J. S. Dyck, and C. Burda, Angew. Chem. Int. Ed. **45**, 5656 (2006).
[17]L. D. Hicks and M. S. Dresselhaus, Phys. Rev. B **47**, 16631 (1993).
[18]D. Kong *et al.*, ACS Nano **5**, 4698 (2011).
[19]G. R. Waitkins and C. W. Clark, Chem. Rev. **36**, 235 (1945).
[20]S. Sun, Y. Sun, Z. Liu, D.-I. Lee, S. Peterson, and P. Pianetta, Appl. Phys. Lett. **88**, 021903 (2006).
[21]L. He *et al.*, J. Appl. Phys. **109**, 103702 (2011).
[22]See supplementary material at http://dx.doi.org/10.1116/1.4724302 for detailed information on LER, Cl-termination of substrates and evidence of HSQ binding.
[23]T. Low, M.-F. Li, G. Samudra, Y.-C. Yeo, C. Zhu, A. Chin, and D.-L. Kwong, IEEE Trans. Electron Devices **52**, 2430 (2005).
[24]J. Falkenhagen, H. Jancke, R.-P. Krüger, E. Rikowski, and G. Schulz, Rapid Commun. Mass Spectrom. **17**, 285 (2003).
[25]Y. Wang, F. Xiu, J. Zou, K. L. Wang, and A. P. Jacob, Appl. Phys. Lett. **96**, 051905 (2010).
[26]D. L. Olynick, B. Cord, A. Schipotinin, D. F. Ogletree, and P. J. Schuck, J. Vac. Sci. Technol. B **28**, 581 (2010).
[27]M. G. Albrecht and C. Blanchette, J. Electrochem. Soc. **145**, 4019 (1998).
[28]J. Matijasević, N. Hassler, G. Reiter, and U. Peter Fringeli, Langmuir **24**, 2588 (2008).
[29]H. Kosslick, V. A. Tuan, R. Fricke, Ch. Peuker, W. Pilz, and W. Storek, J. Phys. Chem. **97**, 5678 (1993).
[30]M. J. Loboda, C. M. Grove, and R. F. Schneider, J. Electrochem. Soc. **145**, 2861 (1998).
[31]S. K. Mishra, S. Satpathy, and O. Jepsen, J. Phys. Condens. Matter **9**, 461 (1997).
[32]N. Bansal *et al.*, Thin Solid Films **520**, 224 (2011).